Analysis of Corn Deterioration Due to Molding Using Surface-Enhanced Raman Spectroscopy

Xiaoyan Wei,[a] Guifang Wu,[a,]* Pengcheng Qiu,[b,]* Huihe Yang,[a] Shubin Yan,[a] Jianing Di,[a] Xiangpeng Zhao,[a] Feixu Zhang,[a] and Hongda Zhang [a]

Efficient and rapid identification of corn mildew levels is essential for proper storage and transportation. This study utilized surface-enhanced Raman spectroscopy (SERS) to obtain Raman spectral fingerprints of moldy corn, combined with multi-class support vector machines (SVM) for rapid detection. Spectral data were preprocessed using the Savitzky-Golay smoothing method, and principal component analysis (PCA) was applied to extract the top five components. Feature peaks were identified using partial least squares discriminant analysis (PLS-DA) regression coefficients, supplemented by manual selection, resulting in eight characteristic wavenumber peaks (482, 878, 1046, 1082, 1220, 1276, 1452, and 1590 cm^{-1}). These features were used for clustering analysis, followed by SVM classification to distinguish mildew levels. The model achieved a 100% recognition rate, validated by cross-validation and confusion matrix analysis. The findings demonstrate that SERS combined with SVM enables precise differentiation of mildew levels, providing reliable support for Raman spectroscopy in fungal detection and grain safety monitoring.

DOI: 10.15376/biores.20.1.1860-1871

Keywords: Moldy corn; Raman spectroscopy; Principal component analysis (PCA); Partial least squares Regression (PLS-Regression); Support vector machine (SVM)

*Contact information: a: College of Mechanical &Electrical Engineering, Inner Mongolia Agricultural University, Hohhot, 010018, P.R. China; b: Ordos Agricultural and Livestock Products Quality and Safety Center, Ordos, 017000, P.R. China; *Corresponding authors: wgfsara@126.com; 26286496@qq.com*

INTRODUCTION

Corn is one of the world's primary feed crops, playing a vital role in enhancing agricultural and livestock production efficiency, ensuring food security, and supporting sustainable agricultural development. Additionally, corn is a key source of nutritional value in both crop and livestock systems. It is rich in crude fiber and possesses a well-balanced amino acid profile, making it widely used in both food and animal feed. The germ tissue is highly porous, exhibiting strong moisture absorption properties, and is abundant in carbohydrates (Liu *et al.* 2017). However, corn is prone to contamination during its growth, harvest, storage, and transportation, which can pose significant threats to animal health and food safety. Therefore, preventing contamination in corn feed and ensuring its quality and safety are critical for improving livestock productivity and ensuring food security. Effective contamination prevention requires sound agricultural management, stringent control over storage and transportation processes, and the adoption of advanced detection technologies for monitoring and analyzing contaminants.

Corn feed is susceptible to contamination by aflatoxins, such as aflatoxin B1, and mycotoxins such as deoxynivalenol (DON), produced by fungi such as *Aspergillus* and

Fusarium species. These mycotoxins are toxic secondary metabolites produced by various fungi, including *Aspergillus*, *Penicillium*, and *Fusarium* species (Girolami *et al.* 2022), and they thrive in environments characterized by high temperature and humidity (Adeyeye 2016). Moreover, some mycotoxins, such as aflatoxins, are heat-resistant and widely distributed. Their stable properties make them difficult to monitor, thus posing a significant threat to the livestock industry.

Traditional detection methods for mycotoxins primarily include enzyme-linked immunosorbent assay (ELISA), high-performance liquid chromatography (HPLC), and gas chromatography (GC). For instance, some researchers have utilized ELISA and HPLC-tandem mass spectrometry (HPLC-MS) to detect two mycotoxins, zearalenone (ZEN) and T-2 toxin, in corn. The results showed that both methods successfully detected zearalenone (ZEA) in feed corn with 100% accuracy. The analysis further indicated that ELISA, with its simple sample preparation and rapid detection speed, is suitable for high-throughput testing. However, it is prone to false positives due to interferences. In contrast, HPLC-MS, although more complex, costly, and requiring higher operational expertise, offers more stable and accurate results (Zhong *et al.* 2019). Additionally, researchers have developed an indirect competitive ELISA to detect deoxynivalenol (DON) in wheat. The results demonstrated that the mouse polyclonal antibody against DON exhibited specific reactivity with 3-acetyl-DON and T-2 toxin. The recovery rate of DON in grains ranged from 82% to 93%, and the linear detection range for DON in grain samples was 0.01 to 100 μg/mL (Fang *et al.* 2011).

These traditional methods typically involve extensive sample preparation, including toxin extraction from the matrix, purification to remove interfering substances prior to detection, and the use of appropriate instrumentation for quantification (Martinez and He 2021). These complex processes are time-consuming, costly, and may result in cross-reactivity and sensitivity issues. Since these methods often rely on reporter molecules that either bind to the target analyte or react with it, false positives may occur, leading to detection failures (Zhang *et al.* 2023). Under restricted detection conditions, these methods may fail to meet the demands for rapid, low-cost testing. Therefore, the development of portable and time-efficient on-site detection tools would be beneficial for corn feed testing.

This manuscript utilizes fluorescence immunoassay-based point-of-care testing (POCT) to measure the levels of mycotoxins in contaminated corn. The results indicate the presence of two mycotoxins, zearalenone (ZEN) and vomitoxin (DON), with toxin concentrations serving as a reference for the degree of corn contamination, which also provides supporting evidence for subsequent Raman spectroscopy analysis. POCT uses portable analytical instruments and corresponding reagents to rapidly obtain test results. It is time- and location-independent, easy to operate, cost-effective, and requires minimal sample preparation (Suo *et al.* 2023), enabling efficient and rapid measurements.

The principle of fluorescence immunoassay is based on the highly specific binding between antigens and antibodies to detect target substances. The fluorescence signal generated by the antigen-antibody complex is proportional to the concentration of fungal toxins, allowing for trace detection (Wang *et al.* 2020). This technique offers reliable and accurate detection of low-concentration targets, demonstrating excellent sensitivity and reproducibility.

In recent years, surface-enhanced Raman scattering (SERS) has become a powerful analytical technique for the rapid and sensitive detection of various contaminants (Gabbitas *et al.* 2023).

Raman spectroscopy is an optical technique used to measure the vibrational energy

of chemical bonds in biomolecules. It provides rapid, non-destructive molecular structural information for both cells and extracellular compounds, without the need for reagents, and sample preparation is simple, even for a variety of biological samples (Hanlon *et al.* 2000).

Surface-enhanced Raman spectroscopy (SERS) has found widespread application in agricultural and by-product safety testing due to its high sensitivity, molecular recognition specificity, and ability for rapid, real-time detection (Li *et al.* 2023). Excitation of localized surface plasmon resonance (LSPR) generates a strong electromagnetic field, and when the sample is placed on a roughened noble metal nanoparticle substrate, the Raman signal is significantly enhanced (Haynes *et al.* 2005). SERS combines Raman spectroscopy with nanotechnology to offer unique chemical and biochemical fingerprints for low-concentration analytes (Gao 2023). This technique, valued for its narrow peak shapes and high resolution in Raman spectra, increasingly provides detailed information on the molecular composition and conformation of samples (Gao *et al.* 2024).

Currently, much of the research on SERS technology focuses on the development of specialized SERS-active substrates, which requires highly specialized skills and advanced equipment, thus limiting its widespread adoption and practical applications (Gabbitas *et al.* 2023).

Although numerous studies have focused on the detection of mycotoxins in maize, and traditional detection methods such as enzyme-linked immunosorbent assay (ELISA), high-performance liquid chromatography (HPLC), and gas chromatography (GC) have seen widespread application to some extent, these methods are often hindered by challenges such as interference from complex sample matrices, false-positive results, lengthy sample preparation processes, and high costs. In particular, there is still a lack of convenient, efficient, and highly sensitive technologies for the rapid and on-site detection of mycotoxins in maize feed. Existing detection methods rely on sample pretreatment and labeling processes, which may introduce errors and reduce the accuracy of the results. Therefore, the current research has yet to fully address the challenge of achieving high-sensitivity, low-cost, label-free, and high-throughput rapid detection in complex samples.

This study combined fluorescent immunoassay with surface-enhanced Raman spectroscopy (SERS) to explore the application of a label-free SERS-based detection method for mycotoxins in maize. By using colloidal silver nanoparticles as the SERS substrate and employing multivariate statistical analyses such as principal component analysis (PCA) and support vector machine (SVM) pattern recognition, the work was successful in developing a model for determining the degree of maize contamination. This approach not only overcomes the limitations of conventional methods but also demonstrates the potential of SERS technology for rapid, portable, and sensitive detection, particularly in complex sample environments.

EXPERIMENTAL

Instruments and Equipment

A fluorescent immunoassay quantitative point-of-care testing (POCT) analyzer (purchased from Shanghai Xiongtu Biotech Co., Ltd.), model XT8201A, and a test strip constant temperature incubator (purchased from Shanghai Xiongtu Biotech Co., Ltd.), model XT8202A, along with a fluorescent immunoassay quantitative test kit were used. The CORA 5001 Raman spectrometer, featuring a spectral range of 100 to 500 cm^{-1}, spectral resolution of 6 to 9 cm^{-1}, and a minimum wavenumber of 100 cm^{-1}, was utilized.

The probe was placed laterally, and samples were placed in the detection vial with the lid closed for testing. The analysis software used were The Unscrambler X version 10.4 and MATLAB R2021a.

Sample Collection and Physicochemical Testing

The samples were collected from a farm warehouse where mold-infected feed corn was stored. Each sample weighed 10 g, with a total of 60 samples numbered from 1 to 60, stored in a cool, dark place.

Before testing, the test strips, extraction solution, sample diluent, and samples were allowed to reach room temperature. The constant temperature incubator and the fluorescent immunoassay quantitative POCT analyzer were preheated for 10 min.

The samples were ground, sifted, and weighed. One gram of the mixed sample was placed in a 10 mL centrifuge tube, and 5 mL of extraction solution was added. The mixture was vortexed for 5 min and then centrifuged at 4000 rpm for 2 min. A 100 µL aliquot of the supernatant was taken and mixed with 600 µL of sample diluent. Then it was set aside for testing. Once the incubator stabilized at 37 °C, the testing began. The ID card was inserted into the ID slot of the fluorescent immunoassay quantitative POCT analyzer to import the test information. The test strip was placed horizontally on the heating plate of the incubator, and 100 µL of the pretreated sample was added to the sample well using a pipette, starting the 6-min incubation timer. After incubation, the test strip was inserted into the analyzer's slot to read the results.

Spectral Detection Process

SERS Substrate preparation

Silver nitrate solution (purchased from Xi'an Tianmao Chemical Co., Ltd.) was used at a concentration of 0.01000 mol/L, grade GR (Guaranteed Reagent), and sodium citrate (purchased from Tianjin Xiangruixin Chemical Technology Co., Ltd.), grade AR (Analytical Reagent). To prepare the silver nanoparticle substrate, the required concentration of silver nitrate solution was prepared by diluting 15 mL of silver nitrate solution with distilled water to a total volume of 150 mL. A 1% mass percent sodium citrate solution was prepared by dissolving 1 g of sodium citrate in 100 mL of water and stirring until dissolved. The diluted silver nitrate solution was then transferred to a flask and heated to boiling on a magnetic stirrer. A total of 4 mL of sodium citrate solution was slowly added while maintaining a stirring speed of 300 rpm. Heating and stirring continued for 20 min until a color change occurred. After the reaction, the solution was allowed to cool to room temperature and stored in a dark place to prevent light exposure.

Test preparation

The samples were crushed using a grinder and sieved through a 40-mesh screen. Exactly 1 g of the sieved sample was placed into a 10 mL test tube, to which 5 mL of universal extraction liquid was added. The mixture was extracted by vortexing for 5 min, followed by centrifugation. 1 mL of the supernatant was then transferred into a measurement vial, to which silver sol enhancement reagent was added. The mixture was thoroughly mixed in preparation for spectral analysis. The form of the sample to be tested was as a mixed solution in a measurement bottle.

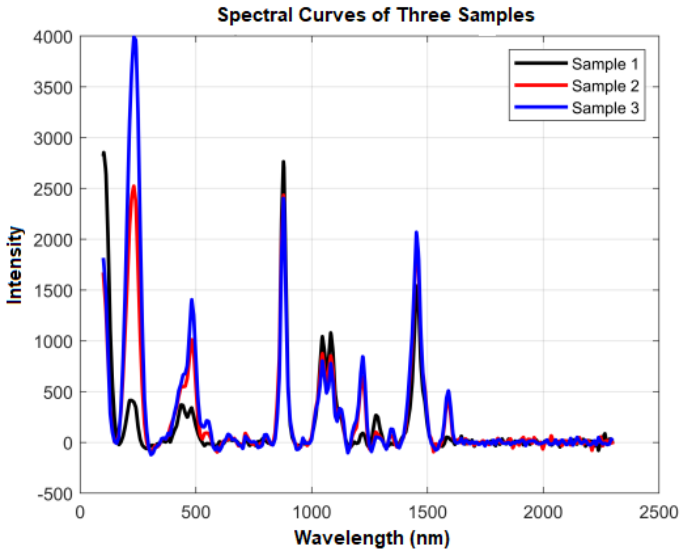

Fig. 1. Typical sample spectrum

Spectral acquisition

The spectrometer was set to the following testing parameters: λ = 1064 nm, p = 450 mW, and t = 10000 ms (auto). Spectral preprocessing included dark background subtraction and baseline correction. The device automatically sampled and saved the results. Each sample was prepared in triplicate to ensure accuracy, and the average value was taken as the final sample's Raman spectral fingerprint. Spectral data were obtained for 60 samples in total. The spectrum of a typical sample is shown in Fig. 1.

RESULTS AND DISCUSSION

Data Analysis

The spectrometer automatically performs dark background subtraction and baseline correction. To mitigate the effects of high-frequency random noise, sample heterogeneity, and light scattering, it is necessary to preprocess the spectra to eliminate random noise. The Savitzky-Golay smoothing method was used for this purpose. The processing was carried out in MATLAB R2021a. The results are shown in Fig. 2.

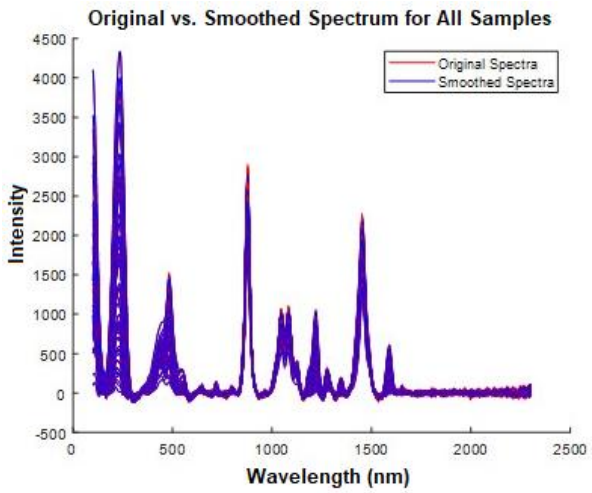

Fig. 2. Spectral smoothing results

Wavelength bands beyond 1700 cm^{-1} contain excessive noise and lack significant peaks, so only data prior to the 1700 cm^{-1} band were retained. A Partial Least Squares Discriminant Analysis (PLS-DA) model was constructed based on Principal Component Analysis (PCA) of the first five principal components and eight characteristic peaks identified using the R-C coefficient method. The 'y' values were assigned such that mild mold contamination was defined as 'sample 1', moderate contamination as 'sample 2', and severe contamination as 'sample 3'. The model involved 57 samples, with 46 used in the modeling set and 11 in the prediction set.

Principal Component Analysis of Spectral Data

After smoothing the spectral data using the Savitzky-Golay (S-G) method, the dimensionality of the data was still too large, necessitating further dimensionality reduction. Principal component analysis reduces dimensions by identifying the directions of maximum variance in the data and constructing a set of orthogonal new axes. PCA captures the directions with the highest variance in the data while attempting to retain as much information as possible. Initially, PCA standardizes the data to neutralize the impact of variable scales by giving each feature the same mean and variance. The standardization formula is as follows,

$$x_{std} = \frac{x-\mu}{\sigma} \quad (1)$$

where μ represents the mean of the features, and σ denotes the standard deviation of the features. The standardized data matrix is expressed as $X(n \times p)$, where n is the number of samples and p is the number of features). Subsequently, the covariance matrix of the standardized data is computed using the following formula.

$$\mathrm{Cov}(X) = \frac{1}{n-1} X^T X \quad (2)$$

The covariance matrix reflects the linear correlation between each pair of features. The next step is to perform eigenvalue decomposition on the covariance matrix to obtain its eigenvalues and eigenvectors. Let the covariance matrix be denoted as C, with its eigenvalues represented by λ and eigenvectors by v, resulting in Eq. 3.

$$C\mathrm{v} = \lambda \mathrm{v} \quad (3)$$

The eigenvalues indicate the variance captured by each principal component, while the eigenvectors represent the directions of these principal components. Based on the magnitude of the eigenvalues, the first *k* eigenvectors were selected as the new basis axes. The data were then projected onto these principal components to obtain the reduced-dimensional data.

The contributions of the principal components obtained after PCA are shown in Table 1.

Table 1. Principal Component Contributions

Principal component	PC-1	PC-2	PC-3	PC-4	PC-5
Cumulative Explained Variance	77.5354	94.7141	96.4960	97.9972	98.5378
Principal component	PC-6	PC-7	PC-8	PC-9	PC-10
Cumulative Explained Variance	98.7261	98.9152	99.0180	99.0909	99.1224

The first five principal components accounted for over 98.5% of the variance. Convex hulls were calculated for each category, and convex polygon boundaries were drawn around each category's perimeter. The classification results are shown in Fig. 3.

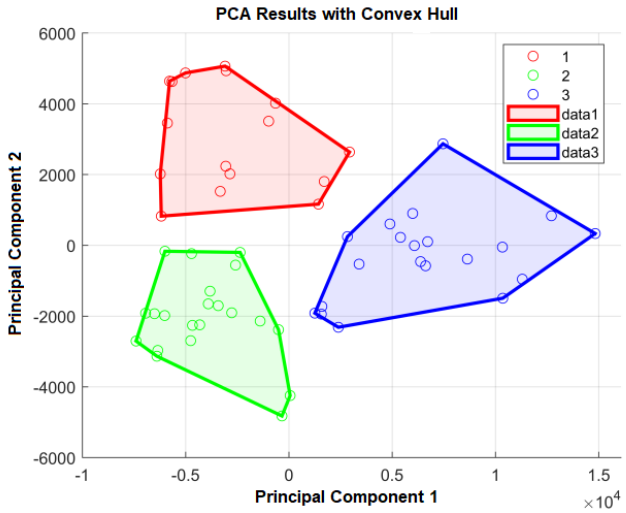

Fig. 3. Principal component analysis (PCA) plot

Partial Least Squares Regression Analysis of Spectral Data

Due to the indistinct separation of edge samples, the model constructed using principal components as inputs for Support Vector Machines demonstrated poor stability. To enhance prediction accuracy, a combination of PCA and Partial Least Squares Discriminant Analysis (PLS-DA) models was used to extract and merge features. Important variables were selected based on the regression coefficients obtained from the PLS regression model, forming a new dataset to build a revised PLS-DA model. The advantage of this model, based on PLS-DA, is that it can detect inter-group variability while reducing the number of variables, allowing for high intra-group variability without needing information about the sample composition to establish the model and distinguish samples (Barker and Rayens 2003). The discriminative effect of the PLS-DA model is illustrated in Fig. 4.

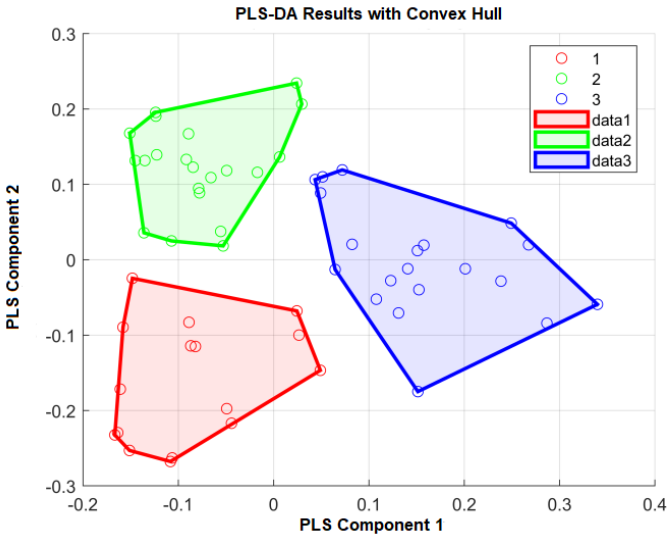

Fig. 4. PLS-DA model discrimination plot

Spectral Peak Feature Analysis

Raman spectroscopy relies on the identification of characteristic peaks. By combining the R-C coefficient method with manual selection, eight characteristic peaks were identified. These peaks are illustrated in Fig. 5. The Raman characteristic peak at 878 cm^{-1} corresponds to CH_2 rocking (Li *et al.* 2019; Zhu *et al.* 2023). The peak at 1046 cm^{-1} is attributed to C-C aromatic ring or C-O stretching vibration, possibly related to in-plane rocking of $-CH_3$ (Tan *et al.* 2015) or C-Cl stretching (Rodriguez *et al.* 2020; Wu *et al.* 2021). The 1220 cm^{-1} peak is associated with C-N stretching, while the 1276 cm^{-1} peak corresponds to β(C-H_2)(ring) and β(C-H) ring deformation (Wu *et al.* 2012). The 1452 cm^{-1} peak is linked to ν(C7=C8), ring deformation (Li *et al.* 2019; Zhu *et al.* 2023), or C-H in-plane bending (Yuan *et al.* 2017). The peak at 1590 cm^{-1} corresponds to the C-C aromatic ring vibration (Agarwal 2006) or β(C-H)(CH_3) and β(C-H)(ring) modes (Wu *et al.* 2012). The 1566 cm^{-1} peak is related to ν($-CH_3$) vibration (Yuan *et al.* 2017).

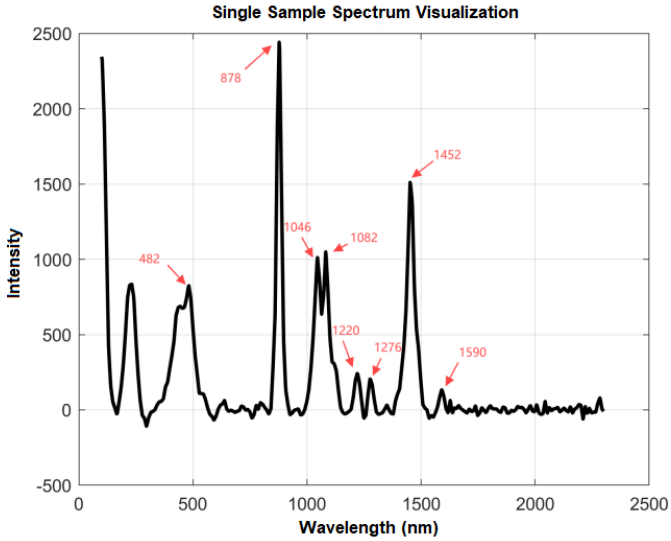

Fig. 5. Characteristic peak identification

Discriminant Analysis Based on Support Vector Machines

The five principal components derived from principal component analysis and the eight characteristic peaks selected *via* the RC coefficient method combined with manual selection were used as inputs for the Support Vector Machine (SVM) algorithm. A one-versus-all SVM approach was implemented using the fitcecoc function in MATLAB, decomposing the multi-class problem into several binary SVM models. The classification of corn mold levels was performed by aggregating the voting results from multiple SVM models, and model classification results were evaluated using a confusion matrix. The algorithm was executed in MATLAB R2021a with the following steps:

(1) Define the known training set as follows:

$$\mathrm{T} = \{(\mathrm{x}_1, \mathrm{y}_1), \ldots, (\mathrm{x}_i, \mathrm{y}_i)\} \epsilon (\mathrm{X} \times \mathrm{Y})^{\ell} \quad (4)$$

where $\mathrm{x}_i \epsilon \mathrm{X} = R^n$; $\mathrm{y}_i \epsilon \mathrm{Y} = \{1, \ldots, \mathrm{M}\}$, $i = 1, \ldots, \ell$.

(2) Perform the following operation on $j = 1, \ldots, M$: treat the j-th class as the positive class and the remaining *M*-1 classes as the negative class, and use the support vector machine to obtain the decision function.

$$f^{\mathrm{j}}(\mathrm{x}) = \mathrm{sgn}\left(\mathrm{g}^j(\mathrm{x})\right) \quad (5)$$

where

$$\mathrm{g}^{\mathrm{j}}(x) = \sum_{i=1}^{l} \mathrm{y}_i \alpha_i^j \mathrm{K}(x, x_i) + b^j \quad (6)$$

(3) Determine the input $\mathcal{X}$ as belonging to the j-th class, where j is the index of the maximum value in $\mathrm{g}^{\ell}(\mathrm{x}),\ldots, \mathrm{g}^{M}(\mathrm{x})$.

(4) For the solution $\alpha = \left(\alpha_1^j, \ldots, \alpha_l^j\right)^{\mathrm{T}}$ of the classification problem, assuming that $\alpha_{\mathrm{k}}^{\mathrm{j}} > 0$ is a component of α, the solution (ω^*, b^*) for (ω, b) can be expressed as

$$\omega^* = \sum_{i=1}^{l} \alpha_i y_i x_i \quad (7)$$

$$b^* = y_k \left(1 - \frac{\alpha_k^j}{\mathrm{C}}\right) - \sum_{i=1}^{l} \mathrm{y}_i \alpha_i^j \mathrm{K}(x_i, x_k) \quad (8)$$

The performance of different kernel functions was compared, and the learning parameters for the SVM were set with a penalty factor c=1000.0. The linear kernel function-based SVM model showed the best classification performance, with confusion matrices displayed in Figs. 6 and 7. The fused model achieved an accuracy of 100% on both the training set and the test set. The results indicate that the feature fusion derived from PCA and PLS analysis effectively distinguishes between different degrees of corn mold.

Fig. 6. Confusion matrix of the training set

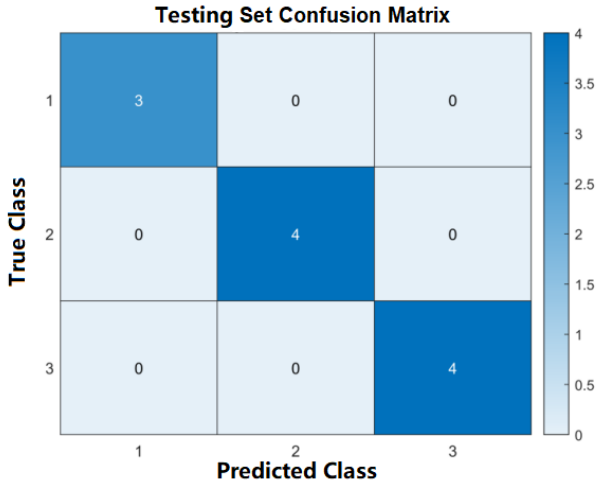

Fig. 7. Confusion matrix of the test set

CONCLUSIONS

1. Fungi secrete enzymes that degrade polysaccharides, such as cellulose, in maize, leading to modifications in its chemical structure. Both deoxynivalenol (DON) and zearalenone (ZEN) molecules feature aromatic ring structures. In Raman spectroscopy, the C–C stretching vibration of the aromatic ring typically appears in the 1400 to 1500 cm^{-1} range. The C=C stretching vibration around 1600 cm^{-1} serves as a characteristic fingerprint peak for deoxynivalenol (DON) and also corresponds to the C=O stretching vibration, which is a key marker for zearalenone (ZEN).
2. This study successfully employed surface-enhanced Raman spectroscopy (SERS) in combination with spectroscopic and chemometric methods to accurately identify the degree of mold deterioration in corn. By applying the Savitzky-Golay smoothing technique for spectral preprocessing and utilizing Principal Component Analysis (PCA) in conjunction with the R-C coefficient method to identify characteristic peaks, key spectral bands were determined at 482, 878, 1046, 1082, 1220, 1276, 1452, and 1590 cm^{-1}, thus significantly enhancing the effectiveness of mold detection.
3. The study further integrated the principal components extracted from PCA with manually selected characteristic peaks to develop a support vector machine (SVM) discriminant model, achieving a recognition accuracy of 100%. This fused discriminant model provides an innovative and efficient approach for future applications of spectroscopic technology in detecting mold contamination, laying a solid foundation for improving food safety monitoring.

ACKNOWLEDGMENTS

This project is supported by the Inner Mongolia Natural Science Foundation (Grant No. 2022MS05049); the National Natural Science Foundation of China (Grant No. 32060414); and the Ordos City Key R&D Program (Grant No. YF20240031).

REFERENCES CITED

Adeyeye, S. A. (2016). "Fungal mycotoxins in foods: A review," *Cogent Food & Agriculture* 2, article 1213127. DOI: 10.1080/23311932.2016.1213127

Agarwal, U. P. (2006). "Raman imaging to investigate ultrastructure and composition of plant cell walls: Distribution of lignin and cellulose in black spruce wood (*Picea mariana*)," *Planta* 224, 1141-1153. DOI: 10.1007/s00425-006-0295-z

Barker, M., and Rayens, W. (2003). "Partial least squares for discrimination," *Journal of Chemometrics* 17, 166-173. DOI: 10.1002/cem.785

Fang, J., Hua, L., Xu, J. H., and Shi, J. R. (2011). "Enzyme-linked immunosorbent-assay for deoxynivalenol (DON)," *Toxins* 3(8), 968-978. DOI:10.3390/toxins3080968

Gabbitas, A., Ahlborn, G., Allen, K., and Pang, S. (2023). "Advancing mycotoxin detection: Multivariate rapid analysis on corn using surface enhanced Raman spectroscopy (SERS)," *Toxins* 15(10), article 610. DOI: 10.3390/toxins15100610

Gao, L. B. (2023). *Study on SERS Detection Methods for Zearalenone and Ochratoxin in Corn*, Master's Thesis, Guizhou University, Guiyang, China. DOI: 10.27170/d.cnki.gjsuu.2023.001731

Girolami, F., Barbarossa, A., Badino, P., Ghadiri, S., Cavallini, D., Zaghini, A., and Nebbia, C. (2022). "Effects of turmeric powder on aflatoxin M1 and aflatoxicol excretion in milk from dairy cows exposed to aflatoxin B1 at the EU maximum tolerable levels," *Toxins* 14, article 430. DOI: 10.3390/toxins14070430

Hanlon, E. B., Manoharan, R., Koo, T. W., Shafer, K. E., Motz, J. T., Fitzmaurice, M., Kramer, J. R., Itzkan, I., Dasari, R. R., and Feld, M. S. (2000). "Prospects for *in vivo* Raman spectroscopy," *Physics in Medicine and Biology* 45(2), R51-R59. DOI: 10.1088/0031-9155/45/2/201

Haynes, C. L., McFarland, A. D., and Van Duyne, R. P. (2005). *Surface-Enhanced Raman Spectroscopy*, ACS Publications, Washington, DC, USA. DOI: 10.1021/ac053456d

Li, J., Yan, H., Tan, X., Lu, Z., and Han, H. (2019). "Cauliflower-inspired 3D SERS substrate for multiple mycotoxins detection," *Analytical Chemistry* 91(6), 3885-3892. DOI: 10.1021/acs.analchem.8b04622

Li, J., Yan, H., Tan, X., Lu, Z., and Han, H. (2019). "Cauliflower-inspired 3D SERS substrate for multiple mycotoxins detection," *Analytical Chemistry* 91, 3885-3892. DOI: 10.1021/acs.analchem.8b04622

Li, Y., Tian, H. Q., Yu, Y., Zhang, J., Zhao, K., Ren, X. G., and Xiao, Z. Q. (2023). "Rapid detection method for pesticide residues in silage corn based on surface-enhanced Raman spectroscopy (SERS)," *Feed Research* (11), 123-128. DOI: 10.13557/j.cnki.issn1002-2813.2023.11.026

Liu, Z. R., Zhang, G. Y., Wang, N. N., and Xu, M. (2017). "Detection and prevention of contamination by main aflatoxin-producing fungi in stored corn," *Plant Protection* 43(6), 46-52+61. DOI: 10.3969/j.issn.0529-1542.2017.06.007

Liu, Z. R., Zhang, G. Y., Wang, N. N., and Xu, M. (2017). "Detection and prevention of contamination by main aflatoxin-producing fungi in stored corn," *Plant Protection* 43(6), 46-52+61. DOI: 10.3969/j.issn.0529 1542.2017.0

Martinez, L., and He, L.-L. (2021). "Detection of mycotoxins in food using surface-enhanced Raman spectroscopy: A Review," *ACS Appl. Bio. Mater.* 4, 295-310. DOI: 10.1021/acsabm.0c01349

Rodriguez, R. S., Szlag, V. M., Reineke, T. M., and Haynes, C. L. (2020). "Multiplex

surface-enhanced Raman scattering detection of deoxynivalenol and ochratoxin A with a linear polymer affinity agent," *Materials Advances* 1, 3256-3266. DOI: 10.1039/d0ma00608d

Suo, Z. G., Niu, X. Y., Wei, M., Jin, H. L., and He, B. S. (2023). "Latest strategies for rapid and point of care detection of mycotoxins in food: A review," *Analytica Chimica Acta* 1246, article 340888. DOI: 10.1016/j.aca.2023.340888

Tan, F., Cai, Q. L., Sun, X. C., Ma, Z. X., and Hou, Z. L. (2015). "Characteristic analysis of cold-region rice leaf blast disease based on Raman spectroscopy," *Transactions of the Chinese Society of Agricultural Engineering* 31(4), 191-196. DOI: 10.3969/j.issn.1002-6819.2015.04.027

Wang, Y., Jiang, J., Fotina, H., Zhang, H., and Chen, J. (2020). "Advances in antibody preparation techniques for immunoassays of total aflatoxin in food," *Molecules* 25(18), article 4113. DOI: 10.3390/molecules25184113

Wu, X., Gao, S., Wang, J.-S., Wang, H., Huang, Y.-W., and Zhao, Y. (2012). "The surface-enhanced Raman spectra of aflatoxins: Spectral analysis, density functional theory calculation, detection and differentiation," *Analyst* 137, 4226-4234. DOI: 10.1039/c2an35378d

Wu, Z., Pu, H., and Sun, D.-W. (2021). "Fingerprinting and tagging detection of mycotoxins in agri-food products by surface-enhanced Raman spectroscopy: Principles and recent applications," *Trends in Food Science & Technology* 110, 393-404. DOI: 10.1016/j.tifs.2021.01.040

Yuan, J., Sun, C., Guo, X., Yang, T., Wang, H., Fu, S., Li, C., and Yang, H. (2017). "A rapid Raman detection of deoxynivalenol in agricultural products," *Food Chemistry* 221, 797-802. DOI: 10.1016/j.foodchem.2016.11.101

Zhang, Y. Y., Zhao, M. J., Liu, C. Y., Ma, K., Liu, T. Y., Chen, F., Wu, L. N., Hu, D. J. and Lv, G. P. (2023)," Comparison of two commercial methods with a UHPLC–MS/MS method for the determination of multiple mycotoxins in cereals," *Food Chem*. 406, article 135056. DOI: 10.1016/j.foodchem.2022.135056Zhu, J., Jiang, X., Rong, Y., Wei, W., Wu, S., Jiao, T., and Chen, Q. (2023). "Label-free detection of trace level zearalenone in corn oil by surface-enhanced Raman spectroscopy (SERS) coupled with deep learning models," *Food Chemistry* 414, article 135705. DOI: 10.1016/j.foodchem.2023.135705

Zhong, X. W., Wang, B. Y., Chen, C., Yang, X. Y., Yang, X. J., Chen, Y., Sun, Z. C., Hua, X. F., Sun, F. H., Zhang, Y. Z., and Tao, L. L. (2019). "Comparative analysis of two mycotoxins in feed corn by ELISA and HPLC-MS," *China Feed* 2019(17), 98-103. DOI: 10.15906/j.cnki.cn11-2975/s.20191722

Article submitted: October 25, 2024; Peer review completed: November 23, 2024; Revised version received: November 29, 2024; Accepted: December 24, 2024; Published: January 10, 2025.
DOI: 10.15376/biores.20.1.1860-1871